

## X-ray absorption spectroscopy of transition-metal doped diluted magnetic semiconductors $Zn_{1-x}M_xO$

J. Okabayashi, K. Ono, M. Mizuguchi, M. Oshima, Subhra Sen Gupta, D. D. Sarma, T. Mizokawa, A. Fujimori, M. Yuri, C. T. Chen, T. Fukumura, M. Kawasaki, and H. Koinuma

Citation: *Journal of Applied Physics* **95**, 3573 (2004); doi: 10.1063/1.1652248

View online: <http://dx.doi.org/10.1063/1.1652248>

View Table of Contents: <http://scitation.aip.org/content/aip/journal/jap/95/7?ver=pdfcov>

Published by the [AIP Publishing](#)

---

### Articles you may be interested in

Coexistence of intrinsic and extrinsic origins of room temperature ferromagnetism in as implanted and thermally annealed ZnO films probed by x-ray absorption spectroscopy

*J. Appl. Phys.* **113**, 183708 (2013); 10.1063/1.4804253

X-ray magnetic dichroism in the (Zn,Co)O diluted magnetic semiconductors from first principle calculations

*J. Appl. Phys.* **111**, 073702 (2012); 10.1063/1.3699276

Probing origin of room temperature ferromagnetism in Ni ion implanted ZnO films with x-ray absorption spectroscopy

*J. Appl. Phys.* **111**, 013715 (2012); 10.1063/1.3676260

Soft-x-ray spectroscopic investigation of ferromagnetic Co-doped ZnO

*J. Appl. Phys.* **99**, 08M111 (2006); 10.1063/1.2165916

Origin of ferromagnetism in Zn O/Co Fe multilayers: Diluted magnetic semiconductor or clustering effect?

*Appl. Phys. Lett.* **85**, 3815 (2004); 10.1063/1.1812844

---



**Not all AFMs are created equal**  
**Asylum Research Cypher™ AFMs**  
**There's no other AFM like Cypher**

[www.AsylumResearch.com/NoOtherAFMLikeIt](http://www.AsylumResearch.com/NoOtherAFMLikeIt)

**OXFORD**  
INSTRUMENTS  
*The Business of Science®*

# X-ray absorption spectroscopy of transition-metal doped diluted magnetic semiconductors $Zn_{1-x}M_xO$

J. Okabayashi, K. Ono,<sup>a)</sup> M. Mizuguchi, and M. Oshima

*Department of Applied Chemistry, The University of Tokyo, Bunkyo-ku, 113-8656, Japan*

Subhra Sen Gupta<sup>b)</sup> and D. D. Sarma

*Solid State and Structural Chemistry Units, Indian Institute of Science, Bangalore 560 012, India*

T. Mizokawa and A. Fujimori

*Department of Complexity Science and Engineering, The University of Tokyo, Bunkyo-ku, 113-0033, Japan*

M. Yuri and C. T. Chen

*Synchrotron Radiation Research Center, Hsinchu 300, Taiwan, Republic of China*

T. Fukumura and M. Kawasaki

*Institute for Materials Research, Tohoku University, Aoba-ku, Sendai 980-8577, Japan*

H. Koinuma

*Department of Innovative and Engineered Materials, Tokyo Institute of Technology, Yokohama 226-8502, Japan*

(Received 1 December 2003; accepted 9 January 2004)

We have investigated the electronic structure of  $Zn_{1-x}M_xO$  ( $M$ : 3d transition metal) by x-ray absorption spectroscopy. Using configuration–interaction cluster-model analyses, electronic structure parameters have been deduced and their chemical trend is discussed. Results show that the  $p$ – $d$  exchange constant  $N\beta$  is negative and large in cases of Mn, Fe, and Co, which is consistent with the enhancement of magnetic circular dichroism. © 2004 American Institute of Physics. [DOI: 10.1063/1.1652248]

## I. INTRODUCTION

Control of both spins and charges of doped carriers has attracted much interest in diluted magnetic semiconductors (DMSs) because the combination of the two degrees of freedom is expected to open up new functionalities in optoelectronic and magnetoelectric devices. Especially, ZnO-based DMSs have high potential for functionalities utilizing the wide band gap (3.4 eV) and the large exciton binding energy (60 meV).<sup>1</sup> If  $Zn_{1-x}M_xO$ , where  $M$  is a 3d transition metal (TM) atom, exhibits ferromagnetism like III–V-based DMSs such as  $Ga_{1-x}Mn_xAs$  and  $In_{1-x}Mn_xAs$ , a transparent magnet can be realized. In fact, a Curie temperature ( $T_C$ ) higher than room temperature was predicted in the case of TM doping in ZnO by a recent theoretical study.<sup>2</sup> While doped Mn into GaAs provides both carriers and local spins at the same time,<sup>3</sup> in the case of  $Zn_{1-x}M_xO$ , it is in principle possible to control the spin and the carrier concentrations independently by co-doping, e.g., Al. In the case of Co doping into ZnO there have been several experiments that suggest a strong  $p$ – $d$  exchange interaction<sup>4,5</sup> and ferromagnetic behavior.<sup>6–8</sup> However, the origin of the ferromagnetism has not been clarified at this moment.

The electronic structure of Mn-doped II–VI based DMS has been extensively studied by photoemission

spectroscopy.<sup>9,10</sup> Utilizing the Mn 3p to 3d resonance photoemission process, the Mn 3d partial density of states (DOS) has been obtained and analyzed using configuration–interaction (CI) cluster-model calculations. In the case of  $Zn_{1-x}Mn_xO$ , the Mn 3d spectral line shape was found to be different from that of  $Zn_{1-x}Mn_xY$  ( $Y = S, Se, \text{ and } Te$ ), which reflects the differences in the electronegativity of the host anions and in the Mn-anion distance.<sup>11</sup> X-ray absorption spectroscopy (XAS) is another powerful technique to investigate the electronic structure of TM compounds using the local process of 2p to 3d absorption. One of the advantages of TM 2p XAS is that the CI analysis of the multiplet structures can give local electronic structure parameters, such as the multiplet and crystal field strengths, more accurately. In this paper, we report on the XAS spectra of  $Zn_{1-x}M_xO$  and the analysis using the CI cluster-model calculation.

## II. EXPERIMENT

Single-crystal thin films were grown on sapphire (0001) substrates at 600 °C under the pressure of  $1 \times 10^{-9}$  Torr by pulsed-laser deposition using KrF excimer laser pulses (248 nm, 5 Hz, 20 ns). A sample library containing several  $Zn_{1-x}M_xO$  thin films with different doping concentrations was fabricated. Details of the sample growth were reported in Ref. 12. X-ray diffraction measurements confirmed the  $c$ -axis-oriented growth of the wurtzite structure free from a second phase. The concentration of TM was determined by electron probe microanalysis (EPMA).

<sup>a)</sup>Present address: Institute of Materials Structure Science, KEK, Tsukuba, Ibaraki 305-0801, Japan.

<sup>b)</sup>Also at: Department of Physics, Indian Institute of Science, Bangalore-560012, India.

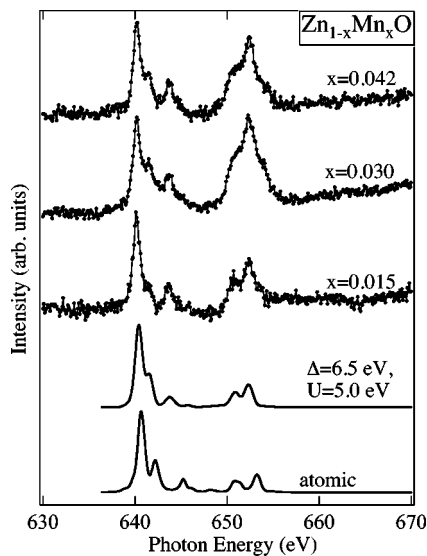


FIG. 1. Experimental Mn  $2p$  absorption spectra for  $\text{Zn}_{1-x}\text{Mn}_x\text{O}$  (dots). Calculated XAS spectra (line) are also shown for  $10Dq=0.5$  eV.

X-ray absorption spectra at the TM  $L_{2,3}$  edge were measured at beamline 11 of Synchrotron Radiation Research Center (SRRRC), Hsinchu, Taiwan. The beamline covers the photon energy range from 400 to 1200 eV. The spectra were measured using the fluorescence mode at room temperature. While the efficiency of fluorescence is low compared with the Auger process after the excitation of the TM  $2p$  electron and the relative intensities of  $L_2$  and  $L_3$  edges may not be reliable due to the self-absorption effect, the fluorescence mode has the advantage that the probing depth is as large as 10–100 nm and is therefore bulk sensitive.

### III. CONFIGURATION-INTERACTION APPROACH

For the analysis of XAS spectra, CI calculations for Mn in ZnO and Co in ZnO were carried out in a  $\text{MO}_4$  ( $M = \text{Mn}$  and  $\text{Co}$ ) cluster, that is modelled as a fragment of the wurzite ZnO structure, with Zn replaced by the TM. The Hamiltonian included the full on-site TM  $3d-3d$  (valence–valence) and  $2p-3d$  (core–valence) Coulomb multiplet interactions, spin–orbit interaction on the TM  $2p$  and  $3d$  manifolds, a tetrahedral ( $T_d$ ) crystal field on the TM, and the hybridization between the TM  $3d$  and O  $2p$  levels. The charge transfer energy is defined by  $\Delta = E(d^{n+1}\bar{L}) - E(d^n)$ , where  $\bar{L}$  denotes a hole in a ligand  $p$  orbital. We have done an all orbital calculation with the full basis, using the Lanczos algorithm. The hybridization between the TM  $3d$  and O  $2p$  levels were parametrized in terms of the Slater–Koster parameters ( $pd\sigma$ ) and ( $pd\pi$ ), where the relation ( $pd\pi$ ) =  $-(pd\sigma)/2$  was used. ( $pp\sigma$ ) and ( $pp\pi$ ) were always set to zero. In all cases, a Gaussian broadening of 0.35 eV was used to simulate instrumental broadening. Details of the calculations were reported in Refs. 13 and 14.

### IV. RESULTS AND DISCUSSION

Figure 1 shows the Mn  $2p$  XAS spectra for  $x=0.015$ , 0.030, and 0.042. The main two peaks are due to the Mn  $2p_{3/2}$  and  $2p_{1/2}$  spin–orbit components. The difference in the

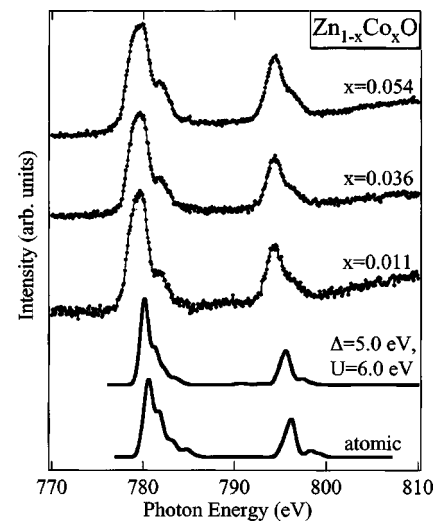


FIG. 2. Experimental Co  $2p$  absorption spectra for  $\text{Zn}_{1-x}\text{Co}_x\text{O}$  (dots). Calculated XAS spectra (line) are also shown for  $10Dq=1.5$  eV.

branching ratio between these spectra comes from the self-absorption of photons emitted from the samples. The line shapes are similar to those reported for  $\text{Zn}_{1-x}\text{Mn}_x\text{Y}$  ( $Y = \text{S}, \text{Se}, \text{and Te}$ )<sup>15,16</sup> and clearly show the  $\text{Mn}^{2+}$  states in the  $T_d$  symmetry.<sup>17</sup> Spectra calculated using the  $\text{MO}_4$  cluster model are shown at the bottom of Fig. 1. The measured XAS spectra have been reproduced using  $\Delta=6.5$ ,  $U=5.0$ , and ( $pd\sigma$ ) =  $-1.6$  eV obtained by the analysis of the Mn  $3d$  partial DOS<sup>11</sup> with the crystal-field splitting  $10Dq$  of 0.5 eV. The calculated spectrum for  $\Delta \rightarrow \infty$ , i.e., in the atomic limit, is also shown. The differences between the two calculations are seen in the positions and the relative intensities of the Mn  $2p_{3/2}$  multiplet peaks. The electronic structure parameters for  $\text{Zn}_{1-x}\text{Mn}_x\text{Y}$  ( $Y = \text{S}, \text{Se}, \text{and Te}$ ) were reported as  $\Delta=3.0$ , 2.0, and 1.5 eV, and ( $pd\sigma$ ) =  $-1.3$ ,  $-1.1$ , and  $-1.0$  eV, respectively, with  $U=4.0$  eV.<sup>18,19</sup> Because of the higher electronegativity of oxygen than the chalcogen atoms,  $\Delta$  is found to be larger than those for  $\text{Zn}_{1-x}\text{Mn}_x\text{Y}$ , following the expected chemical trend.

Figure 2 shows the XAS spectra of Co-doped ZnO. For  $x > 0.050$ , the intensity of the shoulder of the Co  $2p_{3/2}$  peak becomes high. Co  $2p_{1/2}$  also shows a small shoulder structure on the higher photon energy side. Above the solubility limit  $x=0.050$ ,<sup>12</sup> Co or CoO clusters were found to be formed in the crystal, consistent with the reported sample characterization.<sup>12</sup> As shown in Fig. 2, the CI cluster-model calculation reproduced the spectra using the parameters  $\Delta=5.0$ ,  $U=6.0$ , ( $pd\sigma$ ) =  $-1.6$ , and  $10Dq=1.5$  eV. By changing the parameter  $10Dq$ , the line shape drastically changed,<sup>17</sup> and therefore, it was necessary to treat the crystal-field splitting parameter explicitly. This confirms that Co atoms are doped into the Zn site and are tetrahedrally coordinated by ligand oxygen atoms.

Using the above parameters obtained by the cluster-model analysis of  $\text{Zn}_{1-x}\text{Mn}_x\text{O}$  and  $\text{Zn}_{1-x}\text{Co}_x\text{O}$ , we have estimated parameters for other  $\text{Zn}_{1-x}\text{M}_x\text{O}$  compounds through interpolation, as shown in Table I, assuming the expected chemical trend of the parameters. The chemical trend of the parameters in  $\text{Zn}_{1-x}\text{M}_x\text{S}$  and  $\text{Zn}_{1-x}\text{M}_x\text{Se}$  has been

TABLE I. Electronic-structure parameters  $\Delta$  ( $\delta_{\text{eff}}$ ) and  $U$  ( $u$ ), and the exchange constant  $N\beta$  for  $\text{Mn}^{2+}$ ,  $\text{Fe}^{2+}$ , and  $\text{Co}^{2+}$  impurities in ZnO (in eV). ( $pd\sigma$ ) has been fixed to  $-1.6$  eV in the cluster-model analyses and the subsequent estimates of  $N\beta$ .

	$e_{\uparrow}^2 t_{2\uparrow}^3$	$e_{\uparrow}^2 t_{2\uparrow}^3 e_{\downarrow}$	$e_{\uparrow}^2 t_{2\uparrow}^3 e_{\downarrow}^2$
	$\text{Mn}^{2+}$	$\text{Fe}^{2+}$	$\text{Co}^{2+}$
$\Delta$ ( $\delta_{\text{eff}}$ )	6.5 (7.7)	5.5 (7.0)	5.0 (6.8)
$U$ ( $u$ )	5.0 (6.5)	5.5 (7.3)	6.0 (8.0)
$N\beta$	-3.0	-2.7	-3.4

investigated in the previous studies.<sup>19</sup>  $\Delta$  decreases from Ti to Ni due to the difference in the energy position of the TM  $3d$  orbitals. The value of the on-site Coulomb energy  $U$  increases with increasing TM atomic number. The exchange coupling constant  $N\beta$  between the  $\text{TM}^{2+}$   $d$  electrons and the anion  $p$  electrons at the  $\Gamma$ -point valence-band maximum has also been estimated from the obtained parameters assuming that ( $pd\sigma$ ) =  $-1.6$  eV does not change with TM. In the second order of perturbation with respect to the hybridization term, the  $N\beta$  is given by

$$N\beta = -\frac{16}{S} \left( \frac{1}{-\delta_{\text{eff}} + U_{\text{eff}}} + \frac{1}{\delta_{\text{eff}}} \right) \times \left( \frac{1}{3}(pd\sigma) - \frac{2\sqrt{3}}{9}(pd\pi) \right)^2 \quad (1)$$

for  $\text{Mn}^{2+}$ ,  $\text{Fe}^{2+}$ , and  $\text{Co}^{2+}$ , where  $\delta_{\text{eff}} = \Delta_{\text{eff}} - W_p/2$ . Here,  $\Delta_{\text{eff}}$  and  $U_{\text{eff}}$  are, respectively, the charge-transfer energy and the on-site Coulomb energy defined with respect to the lowest term of each multiplet.  $W_p$  is the  $p$ -band width. The intra-atomic  $3d-3d$  Coulomb interaction is expressed by Kanamori parameters  $u$ ,  $u'$ ,  $j$ , and  $j'$  with relationship  $u' = u - 2j$  and  $j' = j$ .<sup>20</sup>  $U$  is given by  $u - 20/9j$ .  $U_{\text{eff}}$  for  $\text{Mn}^{2+}$ ,  $\text{Fe}^{2+}$ , and  $\text{Co}^{2+}$  is expressed by  $u + 4j$ ,  $u + 3j$ , and  $u + 2j$ .  $S$  is the magnitude of the local spin. The  $N\beta$  values thus calculated for several  $\text{TM}^{2+}$  ions are listed in Table I. In the case of  $\text{Zn}_{1-x}\text{Mn}_x\text{O}$ , the  $N\beta$  value has been deduced from the CI cluster-model analysis of the Mn  $3d$  partial density of states.<sup>11</sup> For the  $\text{Mn}^{2+}$ ,  $\text{Fe}^{2+}$ , and  $\text{Co}^{2+}$  impurities, since  $\Delta_{\text{eff}}$  is as large as  $U_{\text{eff}}$ , the contribution of the  $1/(-\delta_{\text{eff}} + U_{\text{eff}})$  term becomes substantial and gives the large  $N\beta$ . The magnetic circular dichroism (MCD) studies of  $\text{Zn}_{1-x}\text{Mn}_x\text{O}$ ,  $\text{Zn}_{1-x}\text{Fe}_x\text{O}$ , and  $\text{Zn}_{1-x}\text{Co}_x\text{O}$  have shown that the MCD signal is negative and strong, which comes from the large Zeeman effect and the strong  $p-d$  hybridization,<sup>5</sup> indicating that the  $p-d$  exchange constant is large. Therefore, the  $\text{TM}^{2+}$  ion is strongly coupled antiferromagnetically with the hole of the host valence band. There are two reasons for the large  $N\beta$  in  $\text{Zn}_{1-x}\text{M}_x\text{O}$  compared with those in  $\text{Zn}_{1-x}\text{M}_x\text{Y}$  ( $Y = \text{S}$  and  $\text{Se}$ ). First, the  $M-O$  and  $M-Y$  distances are different. The shorter distance in  $\text{Zn}_{1-x}\text{M}_x\text{O}$  leads to the larger  $p-d$  hybridization strength. Second, among the II-VI host semiconductors ZnO, ZnS, ZnSe, and ZnTe, a large jump in the electronegativity of anion exists between S and O.

According to the scenario of carrier-induced ferromagnetism, the larger the  $N\beta$  becomes, the higher the  $T_C$  is

expected to be. Theoretical studies on the  $T_C$  of DMS have suggested that  $N\beta$  scales with the bond length between the TM and the ligand atoms, and hence with the  $p-d$  hybridization strength.<sup>21</sup> In fact, in cases of ZnO and GaN, the  $p-d$  hybridization is enhanced because of the short TM-ligand bond length. If holes were doped into  $\text{Zn}_{1-x}\text{M}_x\text{O}$ , high- $T_C$  DMS materials would be realized.

## V. CONCLUSION

In conclusion, we have studied the electronic structure of the TM-doped ZnO using XAS and subsequent CI cluster-model analyses. The XAS spectra have been analyzed using values for the electronic-structure parameters that are consistent with the analysis of the photoemission spectra. The exchange coupling constant  $N\beta$  is estimated to be large using the electronic structure parameters obtained from the CI cluster-model analysis of the XAS spectra. This indicates that  $\text{Zn}_{1-x}\text{M}_x\text{O}$  has a high potential for high- $T_C$  DMS materials if hole doping becomes possible.

## ACKNOWLEDGMENT

This work was partly supported by a Grant-in-Aid for Scientific Research in Priority Area "Semiconductor Nanospintronics" from the Ministry of Education, Culture, Sports, Science and Technology.

- <sup>1</sup>T. Fukumura, Z. Jin, A. Ohtomo, H. Koinuma, and M. Kawasaki, Appl. Phys. Lett. **75**, 3366 (1999); T. Fukumura, T. Yamada, H. Toyosaki, T. Hasegawa, H. Koinuma, and M. Kawasaki, Appl. Surf. **223**, 62 (2003).
- <sup>2</sup>K. Sato and H. Katayama-Yoshida, Jpn. J. Appl. Phys., Part 2 **39**, L555 (2000); **40**, L334 (2001).
- <sup>3</sup>H. Ohno, Science **281**, 951 (1998).
- <sup>4</sup>K. J. Kim and Y. R. Park, Appl. Phys. Lett. **81**, 1420 (2002).
- <sup>5</sup>K. Ando, H. Saito, Z. Jin, T. Fukumura, M. Kawasaki, Y. Matsumoto, and H. Koinuma, Appl. Phys. Lett. **78**, 2700 (2001); J. Appl. Phys. **89**, 7284 (2001).
- <sup>6</sup>K. Ueda, H. Tabata, and M. Kawai, Appl. Phys. Lett. **79**, 988 (2001).
- <sup>7</sup>K. Ando, cond-mat/0208010 (2002).
- <sup>8</sup>H.-J. Lee, S.-Y. Jeong, C. R. Cho, and C. H. Park, Appl. Phys. Lett. **81**, 4020 (2002).
- <sup>9</sup>L. Ley, M. Taniguchi, J. Ghijsen, R. L. Johnson, and A. Fujimori, Phys. Rev. B **35**, 2839 (1987).
- <sup>10</sup>M. Taniguchi, A. Fujimori, M. Fujisawa, T. Mori, I. Souma, and Y. Oka, Solid State Commun. **62**, 431 (1987).
- <sup>11</sup>T. Mizokawa, T. Nambu, A. Fujimori, T. Fukumura, and M. Kawasaki, Phys. Rev. B **65**, 085209 (2002).
- <sup>12</sup>Z. Jin, T. Fukumura, M. Kawasaki, K. Ando, H. Saito, T. Sekiguchi, Y. Z. Yoo, M. Murakami, Y. Matsumoto, T. Hasegawa, and H. Koinuma, Appl. Phys. Lett. **78**, 3824 (2001).
- <sup>13</sup>P. Mahadevan and D. D. Sarma, Phys. Rev. B **61**, 7402 (2000).
- <sup>14</sup>S. Ray, A. Kumar, D. D. Sarma, R. Cimino, S. Turchini, S. Zennaro, and N. Zema, Phys. Rev. Lett. **87**, 097204 (2001).
- <sup>15</sup>W. F. Pong, R. A. Mayanovic, J. K. Kao, H. H. Hsieh, J. Y. Pieh, Y. K. Chang, K. C. Kuo, P. K. Tseng, and J. F. Lee, Phys. Rev. B **55**, 7633 (1997).
- <sup>16</sup>K. Cho, H. Koh, J. Park, S.-J. Oh, H.-D. Kim, M. Han, J.-H. Park, C. T. Chen, Y. D. Kim, J.-S. Kim, and B. T. Jonker, Phys. Rev. B **63**, 155203 (2001).
- <sup>17</sup>G. van der Laan and I. W. Kirkman, J. Phys.: Condens. Matter **4**, 4189 (1992).
- <sup>18</sup>T. Mizokawa and A. Fujimori, Phys. Rev. B **48**, 14150 (1993).
- <sup>19</sup>T. Mizokawa and A. Fujimori, Phys. Rev. B **56**, 6669 (1997).
- <sup>20</sup>J. Kanamori, Prog. Theor. Phys. **30**, 275 (1963).
- <sup>21</sup>T. Dietl, H. Ohno, and F. Matsukata, Phys. Rev. B **63**, 195205 (2001); T. Dietl, H. Ohno, F. Matsukura, J. Cibert, and D. Ferrand, Science **287**, 1019 (2000).